International Journal of Biochemistry and Cell Biology 117 (2019) 105636

Contents lists available at ScienceDirect

International Journal of Biochemistry and Cell Biology

journal homepage: www.elsevier.com/locate/biocel

Hydrogen sulfide protects against cell damage through modulation of PI3K/Akt/Nrf2 signaling

Jiaxin Zhang[a,1], Chaoqun Shi[a,1], Haochen Wang[a,1], Cheng Gao[a], Pan Chang[d], Xiping Chen[a], Haiyan Shan[b,**], Mingyang Zhang[a,c,*], Luyang Tao[a]

[a] Institute of Forensic Sciences, Soochow University, Suzhou, 215123, China
[b] Department of Obstetrics and Gynecology, The Affiliated Suzhou Hospital of Nanjing Medical University, Suzhou, 215000, China
[c] School of Pharmacy, Soochow University, Suzhou, 215000, China
[d] Central Laboratory, The Second Affiliated Hospital of Xi'an Medical College, Xi'an, Shaanxi, 710038, China

ARTICLE INFO

Keywords:
Hydrogen sulfide
Traumatic brain injury
Autophagic cell death
Apoptosis
Oxidative stress
PC12 cell

ABSTRACT

Hydrogen sulfide as the third endogenous gaseous mediator had protective effects against traumatic brain injury-induced neuronal damage in mice. However, the exact pathophysiological mechanism underlying traumatic brain injury is complicated and the protective role of H_2S is not yet fully known. Therefore, we combined the mechanical injury (scratch) with secondary injury including metabolic impairment (no glucose) together to investigate the underlying cellular mechanism of hydrogen sulfide in vitro models of traumatic brain injury. In the present study, we found that H_2S could prevent the scratch-induced decrease in the expression of cystathionine-β-synthetase, a key enzyme involved in the source of hydrogen sulfide, and endogenous hydrogen sulfide generation in PC12 cells. We also found that hydrogen sulfide could prevent scratch-induced cellular injury, alteration of mitochondrial membrane potential, intracellular accumulation of reactive oxygen species and cell death (autophagic cell death and apoptosis) in PC12 cells. It was also found that blocking PI3K/AKT pathway by LY294002, abolished the protection of H_2S against scratch-induced cellular reactive oxygen species level and NRF2 accumulation and function in the nucleus. These results suggest that hydrogen sulfide protects against cell damage induced by scratch injury through modulation of the PI3K/Akt/Nrf2 pathway. This study raises the possibility that hydrogen sulfide may have therapeutic efficacy in traumatic brain injury.

1. Introduction

Traumatic brain injury (TBI) became a worldwide modern healthy problem in society, which is a leading cause of death and leads to long-term disability (Brooks et al., 2013). There is evidence that secondary injury induced by TBI might be specifically associated with oxidative stress due to disturbed equilibrium between oxidant/antioxidant homeostasis that results in permanent brain dysfunction or death (Shen et al., 2016). In order to focus on the role of oxidative stress on neuronal cell death after TBI, we used an in-vitro scratch injury model to mimic the injury condition. The scratch model was first used to study astrocyte behavior after traumatic injury in vitro (Yu et al., 1993). Subsequently, other labs used traumatic scratch injury model to study cell migration and astrogliosis (Etienne-Manneville and Hall, 2001; Gao et al., 2013; Zhu et al., 2007). In neuronal injury, the scratch-injury model is currently widely accepted and used as an in vitro TBI model (Huang et al., 2018; Loov et al., 2013; Ma et al., 2016; Yan et al., 2013). An important advantage of this model is the high reproducibility and is a good tool to screen for possible treatment targets and biomarkers. However, due to its simplicity, the scratch model has limitations in reflecting the complexity of the injured brain (Morrison et al., 2011). Discovering ways to modulate highly complex cellular, neurochemical, and metabolic alterations are needed to attenuate the damaging effects of reactive oxygen species (ROS) and delay many events that contribute to tissue damage (Loane et al., 2015). So as to focus on their fidelity to in vivo pathobiology in vitro models of TBI, we combined the mechanical injury (scratch) with secondary injury including metabolic impairment (no glucose) together to simulate a repetitive head injury model as described previously (Baez-Jurado et al., 2017; Torrente et al., 2014). In vitro models of TBI provides a repeatable and well-controlled

* Corresponding author at: Institute of Forensic Sciences, Soochow University, Suzhou, China.
** Corresponding author at: Department of Obstetrics and Gynecology, The Affiliated Suzhou Hospital of Nanjing Medical University, Suzhou, China.
E-mail addresses: ghostqth@163.com (H. Shan), mingyangzhang@suda.edu.cn (M. Zhang).
[1] Jiaxin Zhang, Chaoqun Shi and Haochen Wang contributed equally.

https://doi.org/10.1016/j.biocel.2019.105636
Received 16 March 2019; Received in revised form 16 October 2019; Accepted 17 October 2019
Available online 22 October 2019
1357-2725/

platform to better understand the underlying mechanisms responsible for cell death and dysfunction after TBI (Morrison et al., 2011).

Hydrogen sulfide (H_2S) displays a large number of biological and physiological effects as the third gasotransmitter, which was produced in the mammalian cells through the enzymatic reactions of cystathionine β-synthase (CBS), 3-mercaptopyruvate sulfurtransferase (3MST) and cystathionine γ-lyase (CSE) (Shefa et al., 2017). The distribution of these enzymes in mammalian cells and tissues is widespread and likely ubiquitous, and CBS is often stated to predominate in the brain (Huang and Moore, 2015). In the adult brain, CBS is highly expressed in some neurons, such as Purkinje cell neurons and hippocampal neurons (Robert et al., 2003) and CBS is the major synthetic enzyme responsible for endogenous H_2S generation in PC12 cells (Tang et al., 2011). It is also expressed in astrocytes, U118 and U373 astrocytoma cells (Enokido et al., 2005; Lee et al., 2009). In addition, the low level of expression of CSE may be localized to glial cells as only CSE, but not CBS, expression was detected in primary cultures of microglial cells (Lee et al., 2006; Zhang et al., 2017b). These results described above confirm that H_2S is synthesized in the brain primarily by the enzyme CBS. Ryo et al reported that CSE was not expressed in PC12 cells and 3-MST pathway is primarily responsible for H_2S production in PC12 cells (Miyamoto et al., 2014). To confirm the expression pattern of the endogenous H_2S producing enzyme in PC12 cells, we examined the expression levels of CSE and 3-MST protein. It was recently demonstrated that H_2S provides protection against oxidative stress through increasing the GSH concentrations, intracellular Trx-1 and nonenzymatic antioxidants production such as nuclear factor (erythroid-derived 2)-like 2 (Nrf2) (Ishigami et al., 2009; Jha et al., 2008; Qu et al., 2008; Yang et al., 2013). Taken together, these findings can serve as evidence that H_2S has potential therapeutic benefits for neural damage due to oxidative stress. Previous studies from our group have demonstrated that endogenous H_2S pathway could be associated with the pathogenesis of TBI and therefore, this pathway may serve as a target for future treatments (Zhang et al., 2014, 2013). Thus, we hypothesized that the protective effect of H_2S on brain damage induced by scratch injury against oxidative stress by targeting the ROS generation and modulating the Nrf2 signaling pathway.

In the present work, we demonstrated that H_2S prevents scratch injury-caused cell death (autophagic cell death and apoptosis) and oxidative stress in PC12 cells and nuclear translocation of Nrf2 involves in this protective action of H_2S. The features of the neuronal damage induced by scratch injury were first investigated. We also investigated the neuroprotective effect of H_2S on oxidative stress and neuronal damage caused by scratch injury in PC12 cells. This is the first study showing that H_2S can suppress scratch injury-induced oxidative stress and autophagic cell death in PC12 cells through the PI3K/Akt/Nrf2 pathway. Our research is aimed to gain a deep understanding of H_2S as an essential mediator of many biological functions and therapeutic potential of H_2S in nervous system disease.

2. Materials and methods

2.1. Materials

Cell viability was measured using a Cell Counting Kit-8 (CCK-8) obtained by Dojindo Molecular Technologies, Inc. (Rockville, MD, USA). The primary antibody to CBS was supplied by Santa Cruz Biotechnology, Inc. (Santa Cruz, CA, USA). The primary antibodies to LC3, P62 were purchased from Abcam (Cambridge, MA, USA). The primary antibodies for PI3K, P-PI3K, Akt, P-Akt, GSK-k3β, P-GSK-k3β, MTOR, P-MTOR, Nrf-2, Histone were from Cell Signaling Technology (Danvers, MA, USA). The primary antibody for β-Actin was from Merck KGaA (Darmstadt, Germany). Reactive Oxygen Assay kit, Mitochondrial Membrane Potential Assay Kit, MDA Elisa kit was supplied by Beyotime Life Science Inc. (Jiangsu, China). DMEM medium and fetal bovine serum (FBS) were supplied by Gibico, BRL (Ground Island, NY, USA). Sodium hydrosulfide (NaHS) was purchased from Sigma and used as exogenous H_2S donor.

2.2. Cell culture

Rat pheochromocytoma PC12 cells were purchased from Chinese Academy of Sciences. Cells were seeded onto a polystyrene culture dish and grown in Dulbecco's modified Eagle's medium-high glucose (DMEM) supplemented with 5% fetal bovine serum (FBS) and 10% horse serum at 37 °C in an atmosphere containing 5% CO_2. The antibiotics penicillin (100 units /mL), streptomycin (100 μg/mL) and glutamine (2 mmol/L) were also included in the medium. Prior to differentiation, the culture medium was exchanged every third day and cultures passaged once or twice a week. For differentiation, 50 ng/ml NGF were maintained for 48 h in a cell incubator at 37°C. Cells between passages 3–8 were treated according to the experiments.

2.3. Cell injury model

Cells were seeded into six-well plates at 6×10^5 cells, 2 ml of medium per well, and grown to 80%–90% confluence after 2 days of culture. PC12 cells cultured on 6 well plates suffered from the scratch injury with 200ul pipette tip making a straight line on a 90% confluent culture of PC12 cells. Multiple scratch injury was performed as T1, T2 and T3 which represent different levels of cell damage. Briefly, confluent cultures were manually scratched using a sterile pipette tip (200 μl), which produced straight vertical and horizontal lines across the culture well. In each well of the 6-well culture plates, 1×1 scratches through the midline were induced in T1 group. In T2 group, 2×2 scratches were induced, producing a 12 mm grid. In T3 group, 3×3 scratches were induced, producing a 9 mm grid. Non-scratched cells were used as control. Culture media were aspirated and cells were washed × 2 in glucose-free EBSS (Earle's balanced salt solution) and added into the serum-free medium (no glucose). Cells were cultured for the indicated duration (0 h, 1 h, 3 h, 6 h, 12 h, 18 h and 24 h). Sodium hydrosulfide (NaHS) as a donor of H_2S was purchased from Sigma-Aldrich (St. Louis, MO, USA) and freshly prepared by dissolving in the saline solution. For treatment, cells were reincarnated with NaHS for 30 min before the scratch injury and continued in coculture for the indicated time with other factors. Matched controls were constantly maintained in DMEM medium under standard normoxic conditions.

2.4. Determination of cell viability

PC12 cells were cultured in 6-well plates at 37 °C in an atmosphere containing 5% CO_2. Cell viability was determined using the cell counting kit-8 (CCK-8) assay (Dojindo Molecular Technologies, Kumamoto, Japan). For ELISA colorimetric assay, 200 μl CCK-8 reagent is added directly to each well, the plates are incubated at 37 °C for 3–4 h and the optical density (OD) in each well at a wavelength of 450 nm is measured in a spectrophotometer (BioTek Instruments, Winooski, VT). The results were expressed as a percentage of the cell survival rate compared with the control. Means of 6 wells OD in the indicated groups were done and repeated three independent times.

2.5. Lactate dehydrogenase release (LDH) assay

Cell injury was analyzed by the release of LDH using LDH-Cytotoxicity Assay Kit (BioVision, Milpitas, CA) according to the manufacturer's instructions. After traumatic scratch injury, the culture medium of each cell group was collected and centrifuged at 10,000 × g. The reaction catalyzed by LDH produced formazan, and the optical density (OD) at 490 nm was measured in a spectrophotometer (BioTek Instruments, Winooski, VT). The results were expressed as a percentage of the cell survival rate compared with the control.

2.6. Nuclear staining for assessment of cell death

Morphological changes and chromosomal condensation in the nucleus of PC12 cells were observed by DAPI and propidium iodide (PI) staining. The PC12 cells were fixed with 4% paraformaldehyde for 10 min. Following three rinses with PBS, the cells were stained with 10 μg/ml DAPI for 10 min. PI (10 mg/ml; Sigma-Aldrich) was diluted in 0.9% NaCl for 40ug/ml. For detection of PI-labeled cells, cells were fixed in ethanol (100%) for 10 min at room temperature, then were stained by PI for 30 min at room temperature and washing 3 times by PBS, and coverslipped with Permount and examined under a Nikon Eclipse Ti-S fluorescence microscope (Nikon Corporation, Tokyo, Japan). Viable cells exhibited a normal nucleus size and uniform fluorescence in the DAPI channel, whereas dead cells exhibited PI/DAPI double-positive staining and condensed nuclei. Colocalization and morphometric measurements were performed using ImageJ 1.6 (NIH).

2.7. Immunofluorescence analysis

PC12 cells in 24-well were fixed with 4% paraformaldehyde for 15 min at room temperature. Following three rinses with PBS, the cells were blocked with the blocking solution (5% normal serum with Triton X-100 and 5% bovine serum albumin) at room temperature for 2 h. After blocking, cells were incubated overnight at 4°C with rabbit polyclonal primary antibodies for anti-LC3 or anti-Nrf2, followed by fluorescein isothiocyanate or Cy3 labeled secondary antibodies for 2 h at room temperature. Following the staining step, cells were washed twice with PBS and incubated with 40ug/ml PI for 30 min at room temperature. After three washes with PBS, the coverslips were mounted using antifade mounting medium and observed with an Eclipse Ti-S fluorescence microscope (Nikon Corporation). Colocalization and morphometric measurements were performed using ImageJ 1.6 (NIH).

2.8. Measurement of H_2S in cell culture supernatant

Culture supernatant from PC12 cells (310 μl) were mixed with 20% trichloroacetic acid (60 μl), 2% zinc acetate (30 μl), 20 mM NNDPD in 7.2 M HCl (40 μl)and 30 mM $FeCl_3$ in 1.2 M HCl (30 μl). H_2S produced in cell culture supernatant can form zinc sulfide when add into zinc acetate, then yield N, N-dimethyl-p-phenylenediamine sulfate (NNDPD) when dissolves in a hydrochloride acid solution if the presence of ferric chloride. Methylene blue will produce and can be quantitated spectrophotometrically (Wang and Yang, 2016). Allow the solutions to stand for at least 15 min, then measure the absorbance of each solution at the wavelength corresponding to maximum absorption (approximately 670 nm), and calculate the concentration of H_2S against a calibration curve of NaHS.

2.9. Intracellular ROS measurement

Dichlorofluorescin diacetate (DCFH-DA), as a fluorescent probe, can cross cell membranes when hydrolyzed to non-fluorescent DCFH by intracellular esterase. According to this, intracellular reactive oxygen species could be detected using DCFH-DA (Chang et al., 2016; Tang et al., 2013). Following scratch injury for 24 h in the presence or absence of 200 μmol/L H_2S, 10 μM DCFH-DA was added to the culture medium and incubated at 37°C for 30 min in the dark. Following the staining step, cells were washed three times with PBS and fluorescence was measured with an excitation/ emission wavelength of 488 nm/ 535 nm under a fluorescence spectrophotometer.

2.10. Determination of mitochondrial membrane potential

Mitochondrial membrane potential was monitored by JC-1 dye, indicated by a fluorescence emission shift from green to red. Cells were stained with 2.5 mg/ml JC-1 for 15 min at 37°C, then washed three times with PBS and mitochondrial membrane potential was observed by the fluorescence microscope. In live cells, JC-1 exists either as a green-fluorescent monomer at depolarized membrane potentials or as a red-fluorescent J-aggregate at hyperpolarized membrane potentials. In order to measure mitochondrial membrane potential, the fluorescent measurement was performed directly with a fluorescence plate reader with red fluorescence in excitation/emission (550 nm/595 nm) and green fluorescence in excitation/emission (485 nm/535 nm). The relative proportions of red and green fluorescence were used to measure the extent of mitochondrial depolarization.

2.11. Measurement of lipid peroxidation, glutathione peroxidase (GSH-Px) and glutathione (GSH)

The content of lipid peroxidation was measured with malondialdehyde (MDA). The cells were then were homogenized and incubated at 4 °C in cell lysis buffer for 20 min. The lysis buffer is containing Tris (50 mmol/L PH 7.5), EDTA (5 mmol/L), sodium dodecyl sulphate (SDS, 1%), NP-40 (1%), Triton X-100(1%), phenylmethanesulfonylfluoride (PMSF, 1 mmol/L), aprotinin (10 μg/mL) and leupeptin (1 μg/mL). MDA concentration in cell homogenates was based on the conjugation ability of MDA with thiobarbituric acid (Gao et al., 2018). The commercial kits were purchased from Beyotime Institute and the maximum absorbance of MDA in cells was measured with a wavelength of 535 nm under a fluorescence spectrophotometer. The commercial kits of GSH-Px and GSH were purchased from Beyotime Institute. A total of 100 μl supernatant was obtained to detect the OD values using a microplate reader according to the instructions, and the activity and content were calculated, respectively. The maximum absorbance in cells was measured with a wavelength of 412 nm under a fluorescence spectrophotometer.

2.12. Western blot analysis

The cells were then were homogenized and incubated at 4 °C in cell lysis buffer for 20 min. The lysis buffer is containing Tris (50 mmol/L PH 7.5), EDTA (5 mmol/L), sodium dodecyl sulphate (SDS, 1%), NP-40 (1%), Triton X-100 (1%), phenylmethanesulfonylfluoride (PMSF, 1 mmol/L), protein (10 μg/mL) and leucopenia (1 μg/mL) (Zhang et al., 2017a). For subcellular fractionation purification, following centrifugation of homogenates from cells at 700 g for 5 min at 4 °C, the pellet (nuclear) was saved and centrifuged at 15 000 g for 10 min to separate pellet (mitochondria) from the supernatant (cytosol). After protein concentration determination in lysates with BCA Protein Assay, 5–20 μg of protein was separated by SDS-PAGE electrophoresis, then transferred from gel to PVDF (polyvinylidene difluoride) membrane at 90v for 1 h. The membrane was then blocked with 5 % nonfat milk and incubated with primary antibody against CBS (1:200; sc-67154; Santa Cruz Biotechnology, Inc., Dallas, TX, USA), 3-MST (1:200; sc-374326; Santa Cruz Biotechnology, Inc., Dallas, TX, USA), CSE (1:200; sc-374249; Santa Cruz Biotechnology, Inc., Dallas, TX, USA), LC3 (1:3,000; ab48394; Abcam, Cambridge, UK), Beclin-1 (1:500; mb0030; Bioworld Technology, USA), sequestration 1 (also known as P62; 1:1,000; ab56416; Abcam), Caspase-3 (1:500; BS1518; Bioworld, USA), Bcl-2 (1:500;BZ00479; Bioworld, USA), PI3K (1:500; 4292; Cell Signal, USA), P-PI3K (1:500; 4228; Cell Signal, USA), Akt (1:500; 4685; Cell Signal, USA), P-Akt (1:500; 4060; Cell Signal, USA), Nrf-2 (1:500; 12721; Cell Signal, USA), Histone (1:500; 3638; Cell Signal, USA) or β-Actin (1:10,000; jla20; Merck KGaA) for overnight. After incubating with anti-rabbit or anti-mouse HRP (horseradish peroxidase)-conjugated secondary antibody, protein was visualized using an enhanced chemiluminescence system (ECL, Pierce Company, USA) and image were obtained by a chemiluminescence imaging system (ChemiScope 5200; Clinx Science Instruments Co., Ltd., Shanghai).

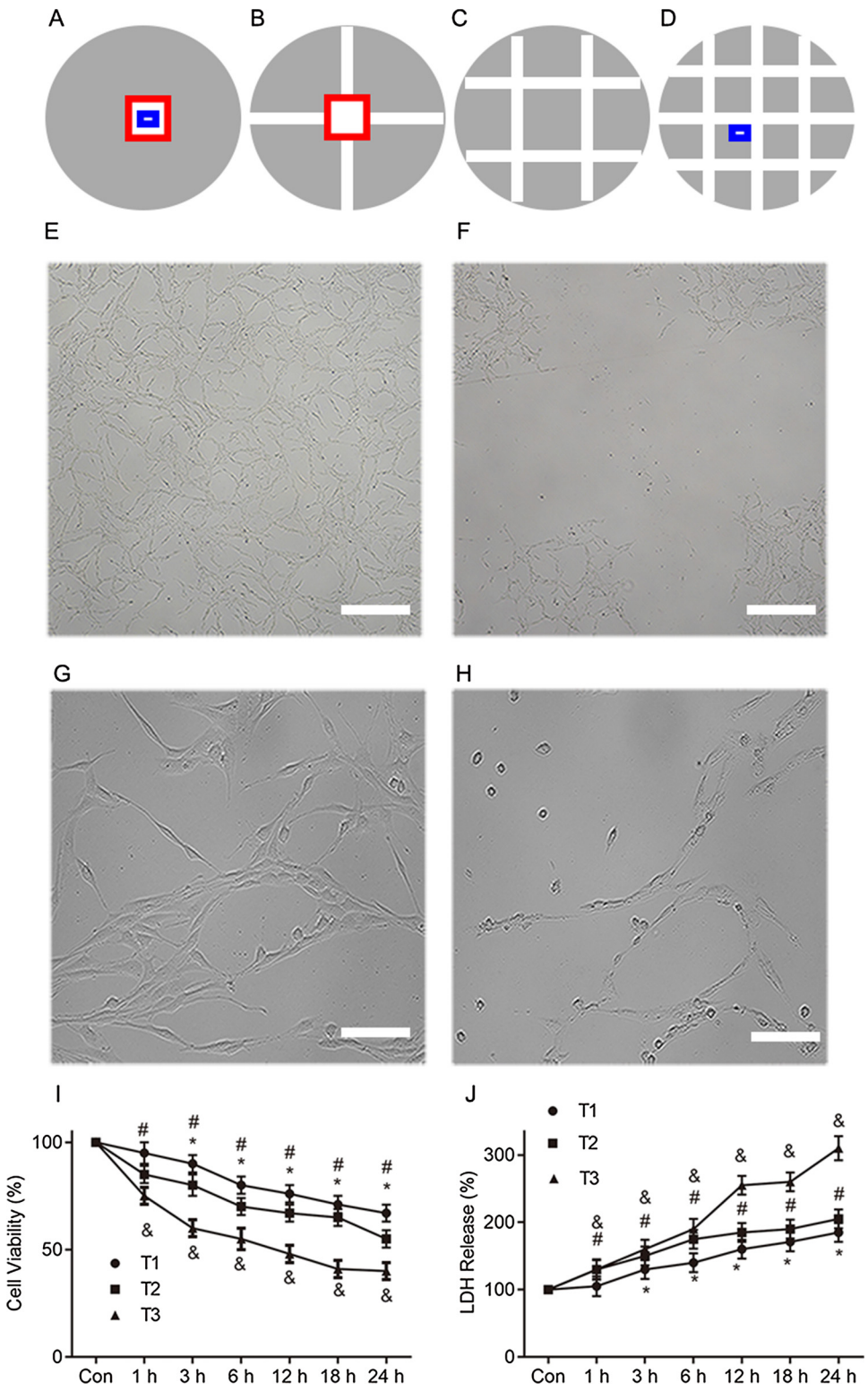

Fig. 1. Time effect of multiple scratch injury on cell viability in PC12 cells. PC12 cells without scratch injury as control (A) and multiple scratch injury were performed as T1 (B), T2 (C) and T3 (D) which represent different levels of cell damage. Representative images of scratch-injured PC12 cells at 24 h in control (E, G). Creating high-quality wounds using tips as seen in (F, H). PC12 cells with multiple scratch tests led to a time-dependent reduction in cell viability (I). LDH release from PC12 cells was determined by a LDH release assay (J). Bar represent means ± SEM of viable cells (n = 6) and expressed as percentages of control values. * $P < 0.05$ T1 group versus control group; # $P < 0.05$ T2 group versus control group; & $P < 0.05$ T3 group versus control group. Scale bars 50 μm (E, F). Scale bars 25 μm (G, H).

2.13. Statistical analysis

All statistical analyses were conducted with SPSS statistical software. Statistical analysis data are expressed as means ± SEM. Comparisons among more than two groups were conducted with analysis of variance (ANOVA) followed by Tukey's post host multiple comparison tests or Student *t*-test (two means comparison). $P < 0.05$ was considered significant. Each experiment consisted of at least three replicates per condition.

3. Results

3.1. Scratch injury influenced the viability of PC12 cells

Scratches were made on the surface of the plate to simulate injury. In order to induce an appropriate injury, multiple scratch injury was performed as T1 (Fig. 1B), T2 (Fig. 1C) and T3 (Fig. 1D) which represent different levels of cell damage. PC12 cells were subjected to multiple scratch tests at a different time (1 h, 3 h, 6 h, 12 h, 18 h, 24 h).

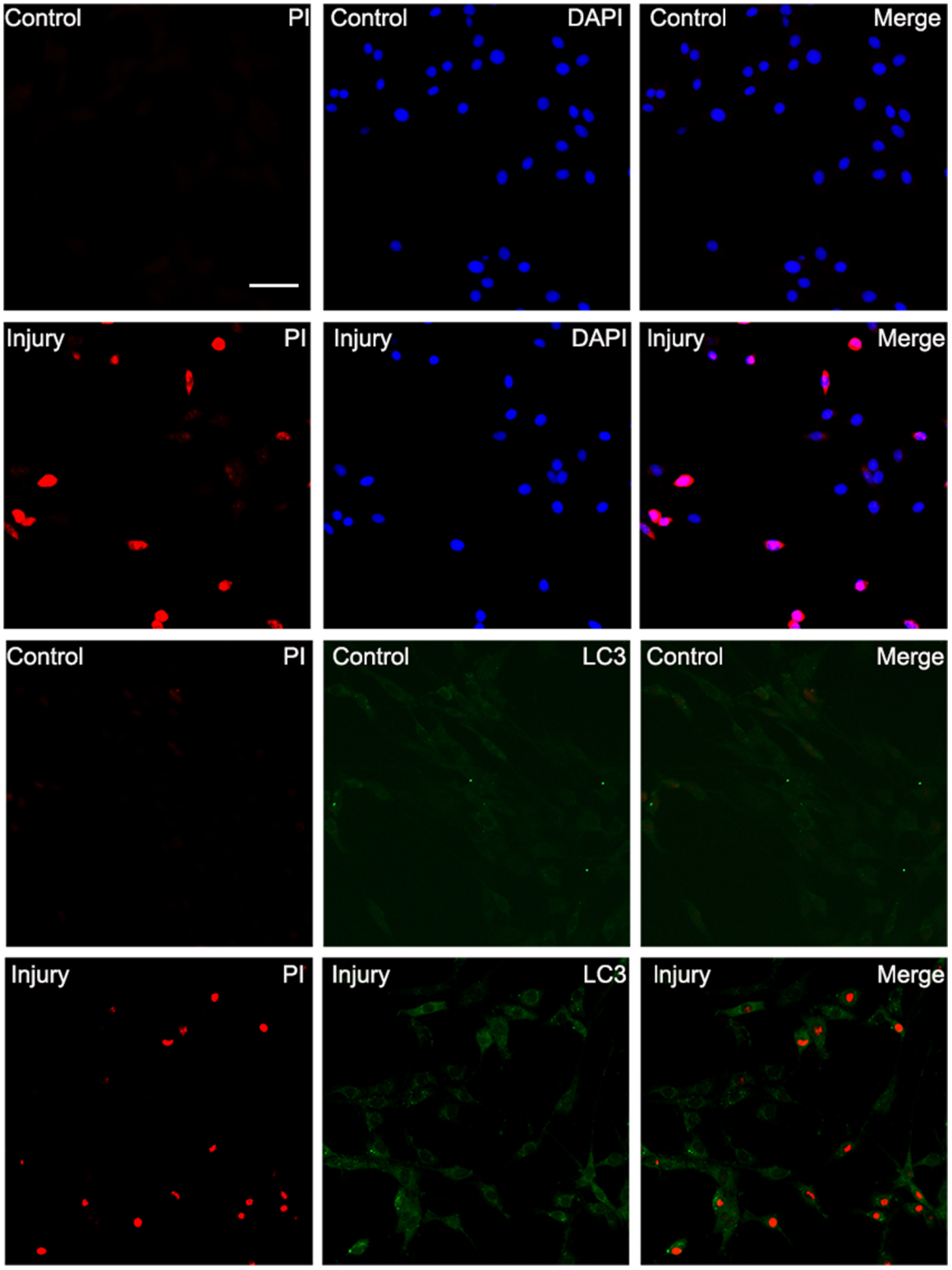

Fig. 2. Effect of scratch injury on cell morphology and autophagic cell death in PC12 cells. PC12 cells were induced by scratch test and then examined by immunostaining and microscopy. Cell death was evaluated by double PI/DAPI staining. Autophagic cell death was evaluated by double LC3/PI staining. Representative images from double-stained fluorescent cells (DAPI, blue; PI, red; LC3, green). Scale bars 30 μm.

Creating wounds using tips create high-quality wounds as seen in (Fig. 1F, 1 H). The cell viability after scratch injury in PC12 cells was evaluated by cell counting kit-8 (CCK-8) assay. As shown in Fig. 1I, multiple scratch tests resulted in a time-dependent decrease in cell viability in PC12 cells (injury vs. control, $p < 0.05$). These results showed the time trend of cell viability when the increment of injury time (Fig. 1G). To determine whether scratch affects cell viability, the LDH assay kit was also used to detect the leakage of LDH from PC12 cells treated with the scratch injury. The results showed that multiple scratch tests resulted in a time-dependent the leakage of LDH from PC12 cells (Fig. 1 J; injury vs. control, $p < 0.05$).

3.2. Scratch injury induces autophagic cell death in PC12 cells

The cell morphology was analyzed by PI/DAPI staining in order to evaluate cell death in PC12 cells. Following DAPI/PI double staining, the nuclei of most cells in the control group are either oval or round and nucleic acid stain can be used with blue-fluorescence (DAPI) and red-fluorescent (PI) labels for analyses. Specifically, cells after scratch injury showed bright, small and round shape condensed nuclei (Fig. 2). To distinguish which type of cell death was induced by scratch, neuronal cultures were examined following staining for PI and for the autophagy marker LC3. The results indicated that LC3/PI double-positive cells existed in the scratch group compared with control (Fig. 2), suggesting that scratch induced autophagic cell death in PC12 cells.

3.3. Hydrogen sulfide prevents scratch-induced inhibition of CBS expression and endogenous H_2S generation in PC12 cells

Western blotting was used to examine the expression levels of CBS as endogenous H_2S-producing enzymes in a control group and injury group induced by scratch injury. The expression levels of CBS protein decreased in a damage degree-dependent manner following injury compared with control (Fig. 3B; injury vs. control, $p < 0.05$). Endogenous H_2S production in PC12 cells after scratch injury was also investigated. As shown in Fig. 3C, the scratch injury resulted in a significant decrease of endogenous H_2S level in a culture medium of PC12 cells (injury vs. control, $p < 0.05$). To investigate the protective effect of H_2S on scratch-induced cell damage, the determination of cell viability was assessed by CCK-8 assay. The damage effects of the scratch injury were significantly suppressed when preconditioning PC12 cells with 100 μmol/L or 200 μmol/L (as the donor of H_2S) for 30 min (Fig. 3D; T3 + NaHS vs. T3, $p < 0.05$). However, the viability of PC12 cells was not a significant change when pretreatment with 200 μmol/L NaHS in normal condition (Fig. 3D; NaHS vs. control, $p > 0.05$). Moreover, pre-treatment with 200 μmol/L of NaHS significantly attenuated scratch injury-induced inhibition of the expression of CBS protein (Fig. 3E; T3 + NaHS vs. T3, $p < 0.05$) and the generation of H_2S (Fig. 3J; T3 + NaHS vs. T3, $p < 0.05$). To confirm the expression pattern of the endogenous H_2S producing enzyme in PC12 cells, we also examined the expression levels of CSE and 3-MST protein. We found that the expression levels of CSE were very low in PC12 cells and there is no change in the expression of MPST and CSE after injury (Fig. 3G; T3 + NaHS vs. T3, $p < 0.05$). These results suggested that CBS is the major synthetic enzyme responsible for endogenous H_2S generation in PC12 cells after the scratch injury. Pretreatment with NaHS significantly attenuated scratch injury-induced inhibition of the expression of CBS protein and the generation of H_2S. However, there was not a significant change in the expression levels of CSE and 3-MST protein after injury when pretreatment with NaHS, suggesting CSE and 3-MST could not be responsible for the increase of H_2S levels when pretreated with NaHS.

3.4. H_2S suppresses scratch-induced autophagic cell death and apoptosis in PC12 cells

To explore the role of H_2S on the autophagy level induced by scratch injury, the autophagy-related proteins such as LC3, Beclin-1 and P62 were detected by Western blot analysis. Scratch injury significantly induced the expression of LC3II and Beclin-1 and suppressed the expression of P62 as illustrated in Fig. 4 (T3 vs. control, $p < 0.05$). However, pretreatment with 200 μmol/L NaHS markedly improved quantification of the P62 concomitant with the downregulation of LC3-II and Beclin-1 in the PC12 cells induced by scratch injury (Fig. 4; T3 + NaHS vs. T3, $p < 0.05$). These results suggested that H_2S could abolish scratch-induced down-regulation of P62 expression and up-regulation of LC3 and Beclin-1 expression. The apoptosis-related proteins such as caspase-3 and Bcl-2 were also detected by Western blot analysis. Scratch injury significantly induced the expression of active caspase-3 and suppressed the expression of Bcl-2 as illustrated in Fig. 4 (T3 vs. control, $p < 0.05$). However, pretreatment with 200 μmol/L NaHS markedly improved quantification of the Bcl-2 concomitant with the downregulation of caspase-3 in the PC12 cells induced by scratch injury (Fig. 4; T3 + NaHS vs. T3, $p < 0.05$). These results suggested that H_2S could abolish scratch-induced apoptosis.

3.5. Hydrogen sulfide reduces scratch-induced intracellular ROS accumulation and lipid peroxidation increase and strengthens the antioxidant capacity in PC12 cells

Because mitochondria are the predominant generators of Reactive oxygen species (ROS) in cells, the level of ROS in the cell may reflect the dysfunction of mitochondrial. DCF-DA can be freely permeable to the cell membrane and used to measure intracellular ROS accumulation. NAC (N-acetyl-L-cysteine) as positive control is frequently employed as a scavenger of ROS. Therefore, we examined the effect of hydrogen sulfide (H_2S) and NAC on ROS levels in PC12 cells induced by scratch injury. The result showed that PC12 cells induced by scratch injury displayed intense fluorescence (2′, 7′-dichlorofluorescein) after staining with DCF dye (Fig. 5D; T3 vs. control, $p < 0.05$). The intracellular accumulation of ROS induced by scratch injury was significantly suppressed when pretreatment with H_2S (Fig. 5E; T3 + NaHS vs. T3, $p < 0.05$) or NAC (Fig. 5F; T3 + NAC vs. T3, $p < 0.05$). Excessive MDA production in PC12 cells induced by scratch injury for 24 h was also observed to 143% of control values (Fig. 5 H; T3 vs. control, $p < 0.05$), suggesting an increase in lipid peroxidation level. When H_2S (200 μmol/L) was present in the media, the level of MDA was significantly decreased compared with the injury group (Fig. 5 H; T3 + NaHS vs. T3, $p < 0.05$). The results indicated a significant reduction in the activity levels of GSH and GSH-Px (Fig. 5 I, 5 J; T3 vs. control, $p < 0.05$), in addition to an increase in the level of MDA following scratch injury. The reduced GSH and GSH-Px activity were attenuated following pretreatment with H_2S (Fig. 5I, 5 J; T3 + NaHS vs. T3, $p < 0.05$).

3.6. The protective effect of hydrogen sulfide on mitochondrial membrane potential depolarization and cell viability induced by scratch injury

To verify mitochondrial membrane potential depolarization in PC12 cells induced by scratch injury, JC-1 dye was used as a mitochondrial membrane potential indicator and can be investigated by fluorescent imaging. When PC12 cells were subjected to scratch injury, the green fluorescence was increased (Fig. 6C; T3 vs. control, $p < 0.05$). But pretreatment with NaHS, the green fluorescence was repressed and the red fluorescence was restored, suggesting that NaHS reduced the changes in mitochondrial membrane potential (Fig. 6D; T3 + NaHS vs. T3, $p < 0.05$). By phase-contrast microscopy, PC12 cells pretreated with 200 μmol/L NaHS appeared longer spindle-like shape, compared with the round to oval-like shape in control PC12 cells subjected to scratch injury for 24 h (Fig. 6E and F). The ratio of red to green fluorescence intensity showed that the protective effect of hydrogen sulfide on mitochondrial membrane potential depolarization induced by scratch injury (Fig. 6G). We investigated thereafter whether NaHS can protect PC12 cells from scratch-induced cell death. Pretreatment with 200 μmol/L NaHS significantly attenuated scratch-induced decrease of cell viability in PC12 cells (Fig. 6H; T3 + NaHS vs. T3, $p < 0.05$).

3.7. The PI3K/AKT//Nrf2 pathway is involved in the regulation of scratch-induced ROS in PC12 cells

To ascertain the possible role of PI3K/AKT/Nrf2 pathways in scratch-induced ROS, we verified the active phosphorylated forms of PI3K, AKT and accumulation of Nrf2 in the nucleus. The active phosphorylated forms of PI3K and AKT were decreased after scratch injury

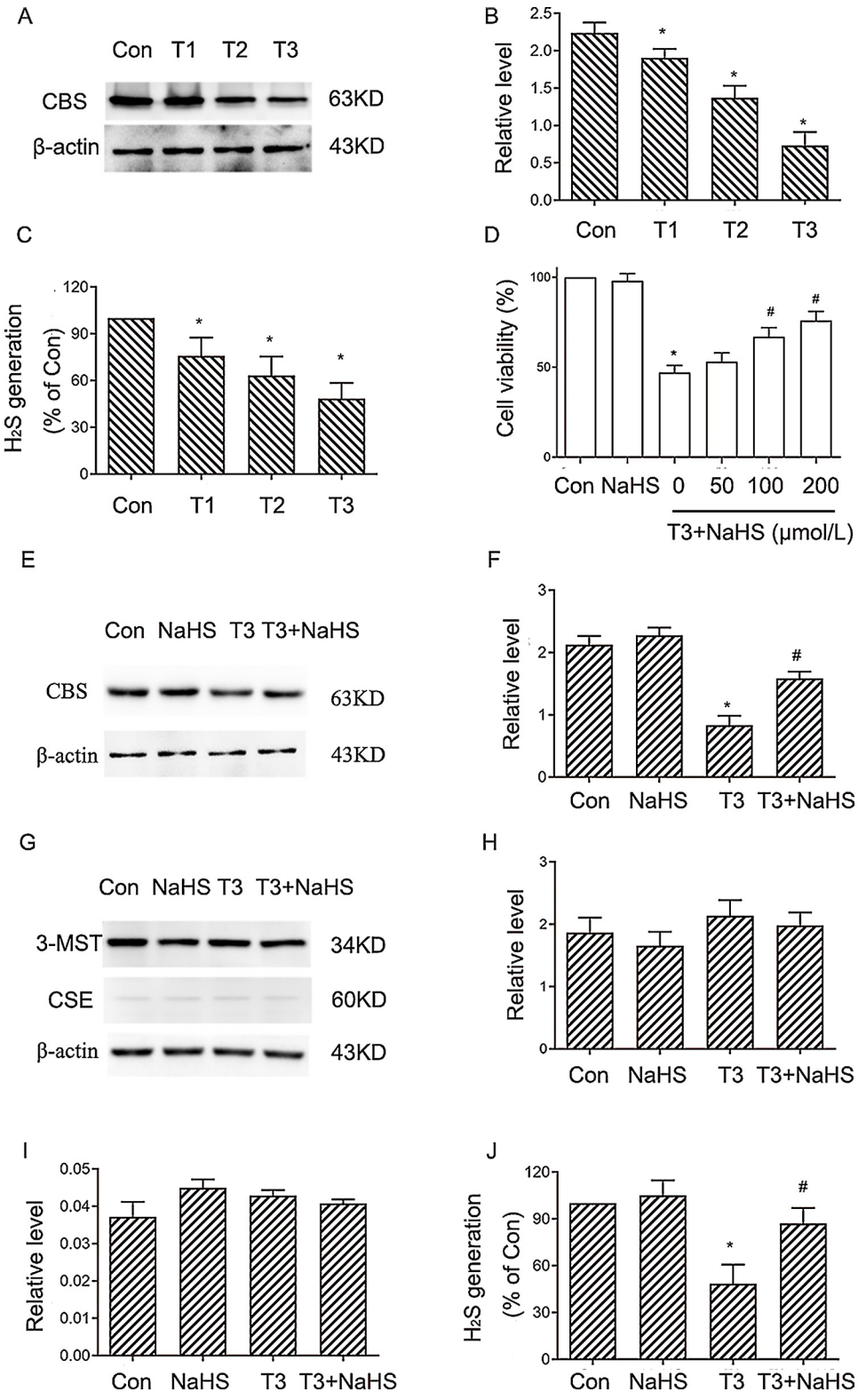

Fig. 3. Effects of Hydrogen sulfide on scratch-induced inhibition of CBS, 3-MST and CSE expression and endogenous H_2S generation in PC12 cells. Cells were subjected to different extent of scratch damage for 24 h and then analyzed by (A) western blotting for CBS. These (T1, T2, T3) represent different levels of cell damage. The relative protein expression of CBS was calculated, with β-actin as the loading control (B). The expression levels of CBS protein decreased in a damage degree-dependent manner following injury compared with control. Representative images and quantification as mean protein levels relative to β-actin ± standard error of the mean (n = 3). *P < 0.05 vs. control. The content of H_2S in culture medium cells was measured by the N, N-dimethyl-p-phenylenediamine sulfate (NNDPD) method as described in Material and Methods (C). PC12 cells were subjected to the scratch injury in the absence or presence of H_2S (50, 100 and 200 μmol/L) for 24 h, and then cell viability was determined by CCK-8 assay (D). When pretreatment with H_2S (200 μmol/L), CBS expression (E) and endogenous H_2S generation (J) in PC12 cells after injury increased. The expression levels of CSE were very low in PC12 cells (G) and there is no change in the expression of 3-MST (H) and CSE (I) after injury. Values are the mean ± SEM (n = 6). *P < 0.05 versus control group, #P < 0.05 versus injury alone group.

in PC12 cells (Fig. 7A and B; T3 vs. control, $p < 0.05$). Nuclear translocation leads to the accumulation of Nrf2 in the nucleus of PC12 cells after injury induced by scratch compared with untreated cells (Fig. 7E and F, 8; T3 vs. control, $p < 0.05$). As shown in Fig. 7, 200 μM NaHS treatment strongly induced the protein expression of the phosphocreatine forms of PI3K and AKT and Nrf2 accumulation in the nuclear (T3 + NaHS vs. T3, $p < 0.05$). To determine how changes in PI3K-Akt signaling, PC12 cells were treated with the PI3K inhibitors, LY294002, at various concentrations. Treatment with LY294002 for 24 h at concentrations higher than 5 μM resulted in a significant decrease in the phosphorylation of

Akt (Fig. 7I). LY294002, as an inhibitor of the PI3K family, were added into the culture media with NaHS, then translocation of Nrf2 from the cytoplasm to nucleus was determined by Western-blot and immunofluorescence and accumulation of ROS within cells was measured by the use of DCF-DA. The down-regulation of ROS level and the

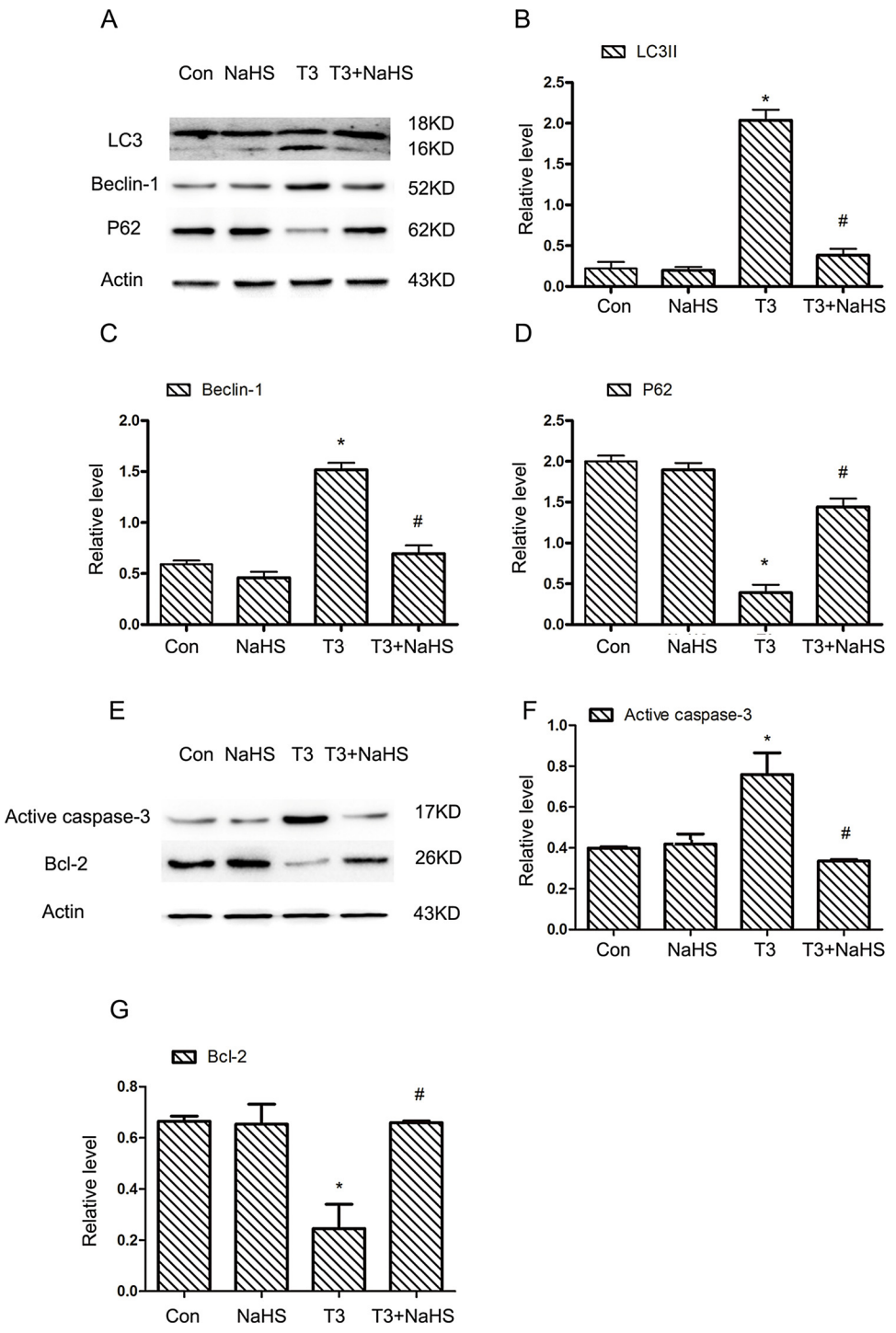

Fig. 4. Effect of hydrogen sulfide on cell death-associated protein expression induced by scratch injury in PC12 cells. Sample immunologic probed for LC3, Beclin-1, P62, Caspase-3, Bcl-2 and β-actin are shown above. The *bar chart* below demonstrates the ratio of LC3 II, Beclin-1, P62, Caspase-3 or Bcl-2 relative to β-actin for different groups. Con denotes control group. Semiquantitative analysis (relative optical density) of the intensity of staining of LC3 II (B), Beclin-1 (C), P62 (D), Caspase-3 (F) or Bcl-2 (G) to β-actin for different concentrations. The data are means ± SEM (n = 3, *P < 0.05, significantly different from the control group, #P < 0.05 versus injury alone group).

nuclear accumulation of Nrf2 induced by NaHS could be effectively suppressed by preincubation with LY294002, as shown in Fig. 7L (T3 + NaHS vs. T3, $p < 0.05$) and Fig. 8.

4. Discussion

In recent decades, more and more attention has been paid to the models of nervous system trauma in vitro (Ma et al., 2012). This is because in vitro cell injury models as a screening tool will allow the identification of new active compounds that may eventually be validated on in vivo traumatic brain injury (TBI) models. Currently, there are still no precise preventive and curative strategies for nervous system trauma and progression is thus also urgently needed to support the development of new therapeutic agents. In vitro cell injury model may also be used to perform a large-scale screen that identified more effective therapeutic strategies (Faden et al., 2005). In this study, we examined the cell damage occurring in cultured PC12 cells when suffered from a scratch assay with metabolic impairment (no glucose) together in a TBI in vitro Model. We demonstrated an injury's severity-dependent and time-dependent effects of the scratch injury on cell viability. We also observed ROS production and the changes in mitochondrial morphology and function induced by scratch assay in traumatic brain like-injury cell model. So far, no study has yet been conducted to investigate whether H_2S could prevent cytotoxicity

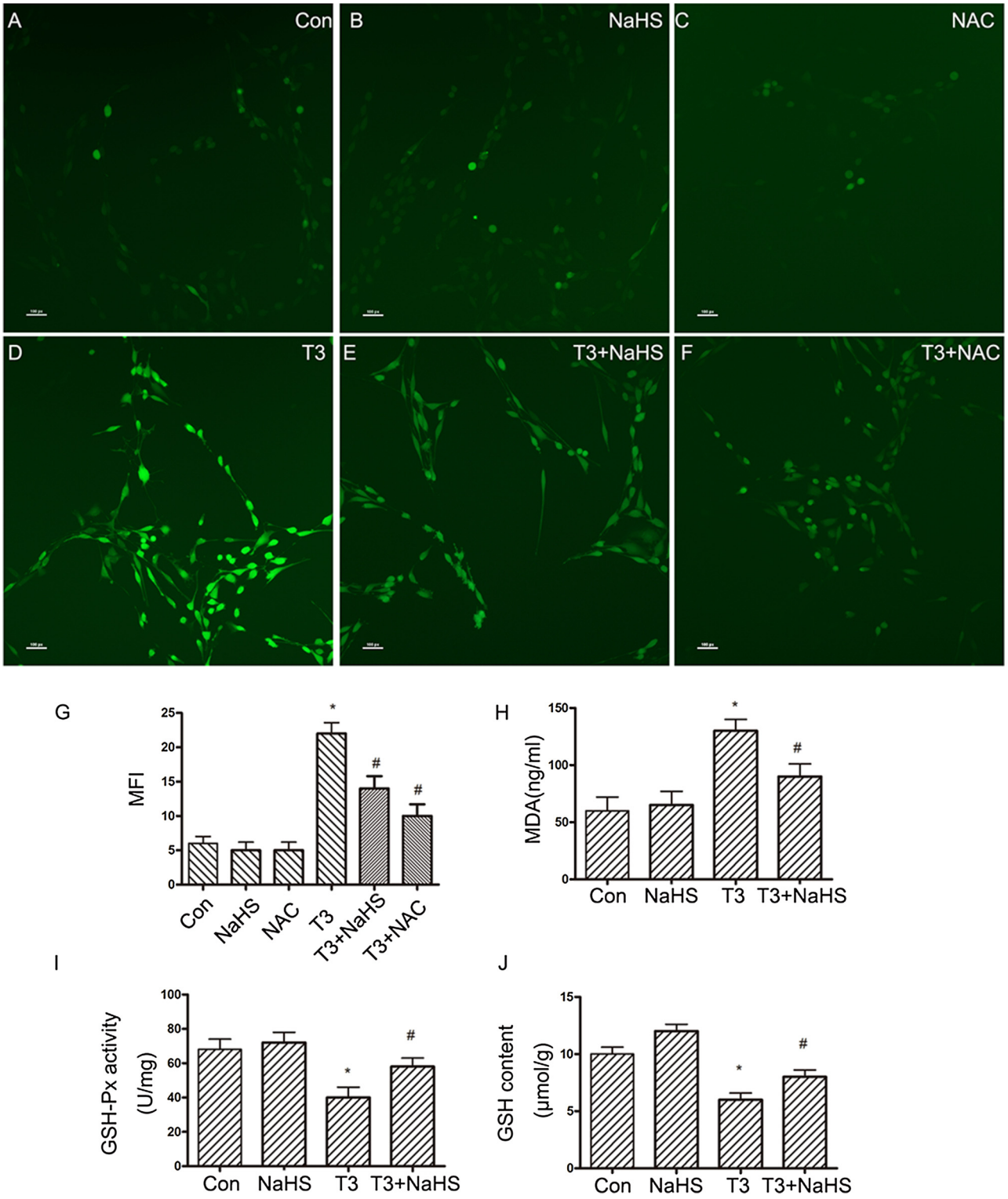

Fig. 5. Protective effect of hydrogen sulfide on scratch-induced intracellular ROS accumulation and MDA formation and the decrease of glutathione peroxidase (GSH-Px) and glutathione (GSH). Intracellular peroxide levels were determined based on the DCF fluorescence, as described in Materials and Methods. Cells were plated and grown for 24 h, then they were exposed to scratch injury in the presence or absence of NaHS. (A) Control; (B) 200 μmol/L NaHS; (C) NAC ; (D) Scratch injury; (E) Scratch injury + 200 μmol/L NaHS; (F) Scratch injury + NAC; (G) The bar chart below demonstrates that the quantitative analysis of median fluorescence intensity. NAC (N-acetyl-L-cysteine) is commonly used to identify and test ROS inducers, and to inhibit ROS. The data are means ± SEM (n = 6, *P < 0.05, significantly different from the control group; #P < 0.05, significantly different from the injury group). Scale bars 50 μm. PC12 cells were subjected to scratch injury in the absence or presence of H_2S (200 μmol/L) for 24 h, and then Malondialdehyde (MDA), a by-product of a free radical attack on lipids, was determined by thiobarbituric acid (TBA) assay. We also investigated the glutathione level after scratch injury and found that the decrease of GSH-Px (I) and GSH (J) in PC12 cells induced by scratch injury for 24 h was also observed. When H_2S was present in the media, the level of GSH-Px and GSH was significantly increased compared with the injury group. Values are the means ± SEM (n = 6). *P < 0.05 versus control group, #P < 0.05 versus injury alone group.

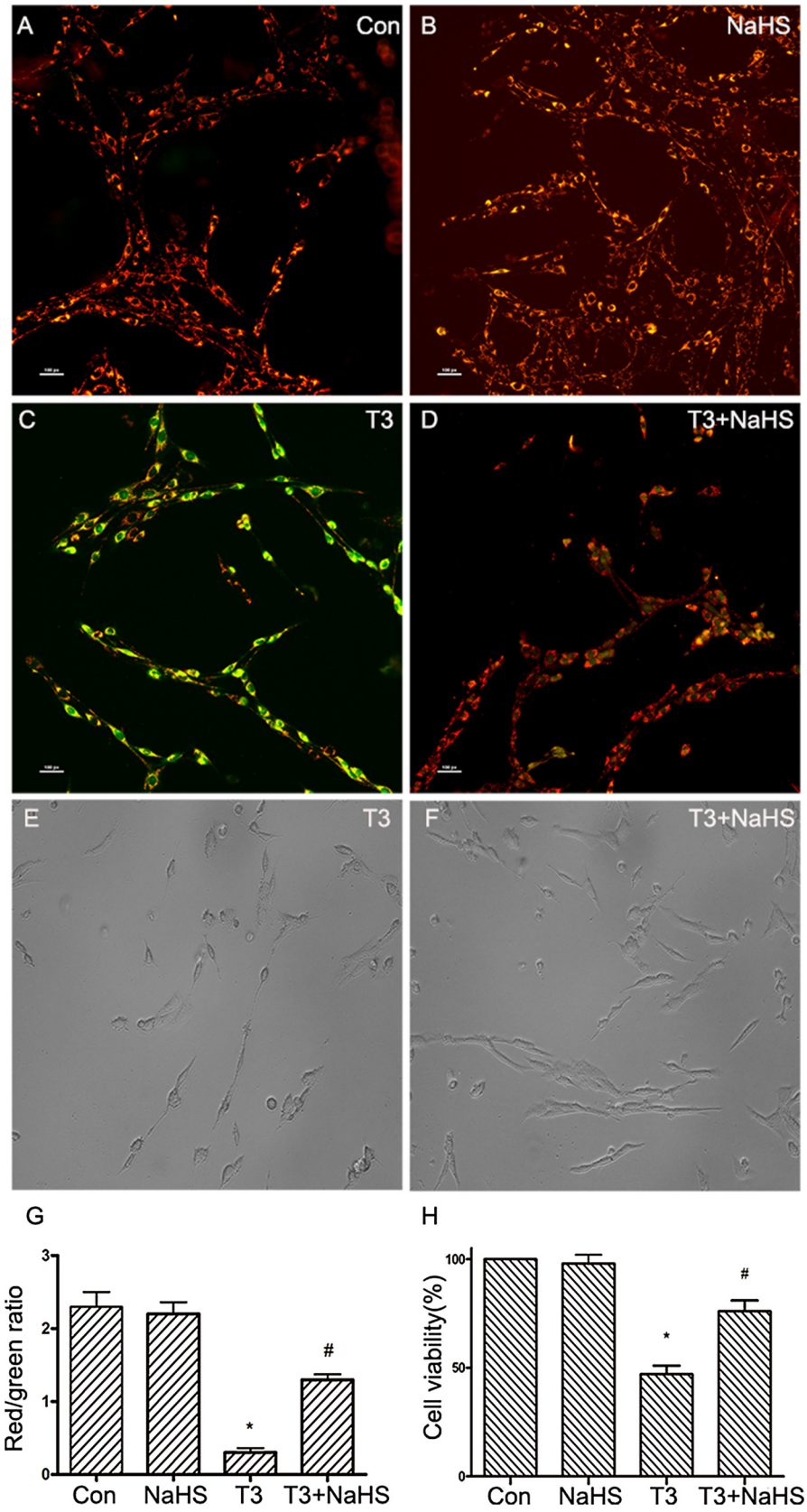

Fig. 6. Effect of hydrogen sulfide on the mitochondrial membrane potential and cell viability induced by scratch injury. JC-1 is an indicator of mitochondria membrane potential. Laser microscope images of JC-1 fluorescence in PC12 cells after 24 h subjected to scratch injury alone or associated with 200 μmol/L NaHS. (A) Control; (B) 200 μmol/L NaHS; (C) scratch injury; (D) scratch injury + 200 μmol/L NaHS. Representative images from phase-contrast microscopy in PC12 cells after 24 h subjected to scratch injury alone or associated with 200 μmol/L NaHS. (E) scratch injury; (F) scratch injury + 200 μmol/L NaHS. The bar chart below demonstrates that the quantitative analysis of Red/Green ratio (G). PC12 cells were pre-treated with 200 μmol/L NaHS, then subjected to scratch injury and cell viability was determined by CCK-8 assay (H). The data are means ± SEM (n = 6, *P < 0.05, significantly different from the Control group; #P < 0.05, significantly different from the injury group). Scale bars 30 μm.

induced by scratch injury in PC12 cells and whether scratch-induced cell death (autophagic cell death and apoptosis) might be attributed to oxidative stress. We found that blocking PI3K/AKT pathway by LY294002, abolished the protection of H_2S against scratch-induced cellular reactive oxygen species level and NRF2 accumulation and function in the nucleus. Taken together, our findings suggested that H_2S suppressed scratch-induced autophagic cell death and apoptosis through decreasing ROS generation via PI3K/Akt/Nrf2 pathway

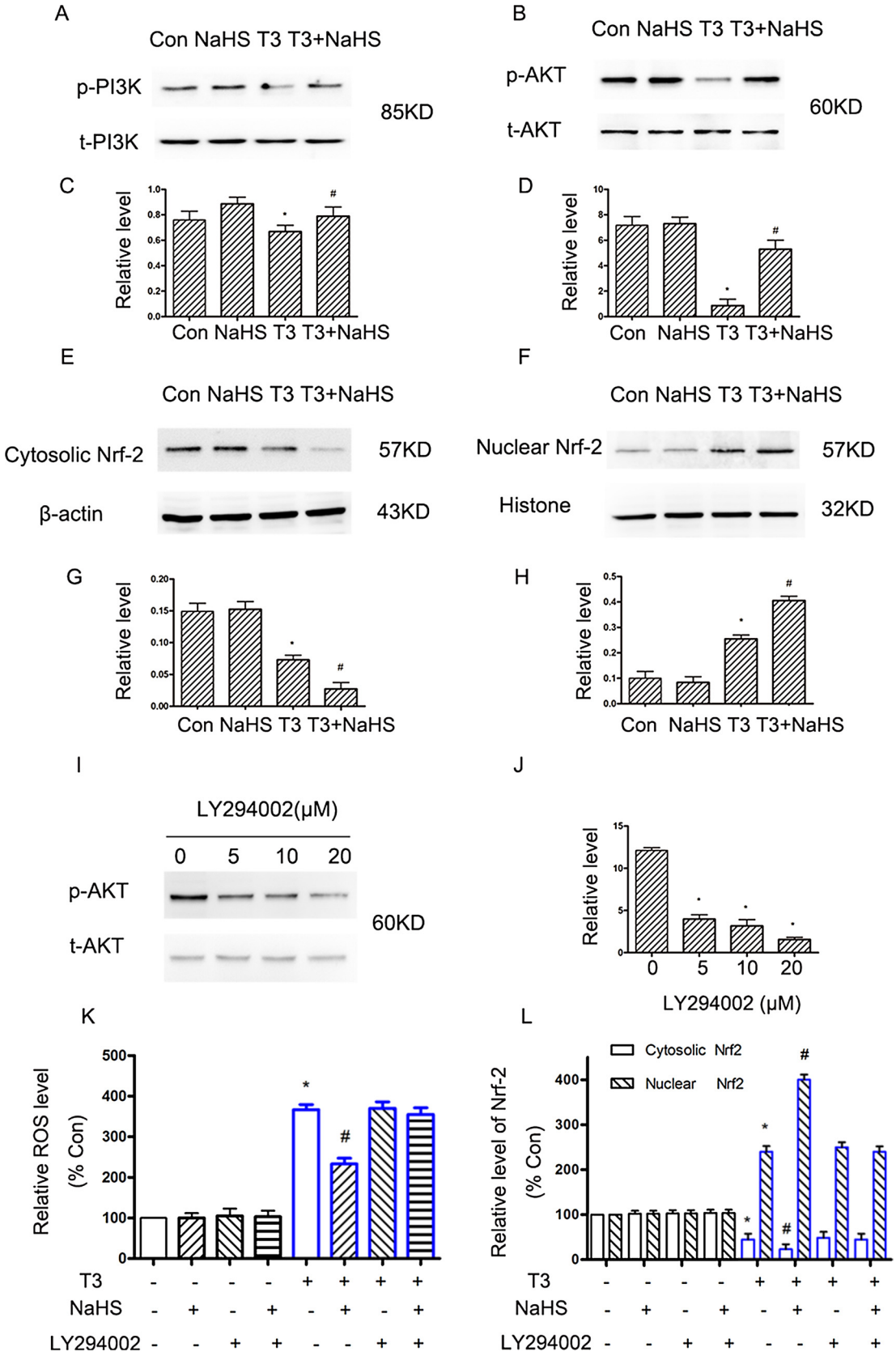

Fig. 7. PI3K, AKT, and Nrf2 signaling pathways participate in the Scratch-induced ROS in PC12 cells. Sample immunologic probed for t-PI3K, p-PI3K, t-AKT and p-AKT are shown (A, B). The bar chart below demonstrates the ratio of p-PI3K relative to t-PI3K or p-AKT relative to t-AKT for scratch injury. Scratch injury significantly decreased the amount of p-PI3K (C) expression and the p-AKT (D) expression. However, co-treatment with 200 μmol/L NaHS significantly abolished the scratch-induced decrease in p-PI3K expression and p-AKT expression (C, D). Nuclear and cytoplasmic extracts were prepared from PC12 treated with NaHS (E, F) and LY294002 (L) analyzed by Western-blot. To determine how changes in PI3K-Akt signaling, PC12 cells were treated with LY294002, as the PI3K inhibitors, at various concentrations (I). The bar chart below demonstrates p-AKT relative to t-AKT at various concentrations of LY294002 (J). ROS accumulation was measured by the use of DCF-DA (K). Con denotes control group. The data are means ± SEM (n = 3, *P < 0.05, significantly different from the control group, #P < 0.05 versus injury

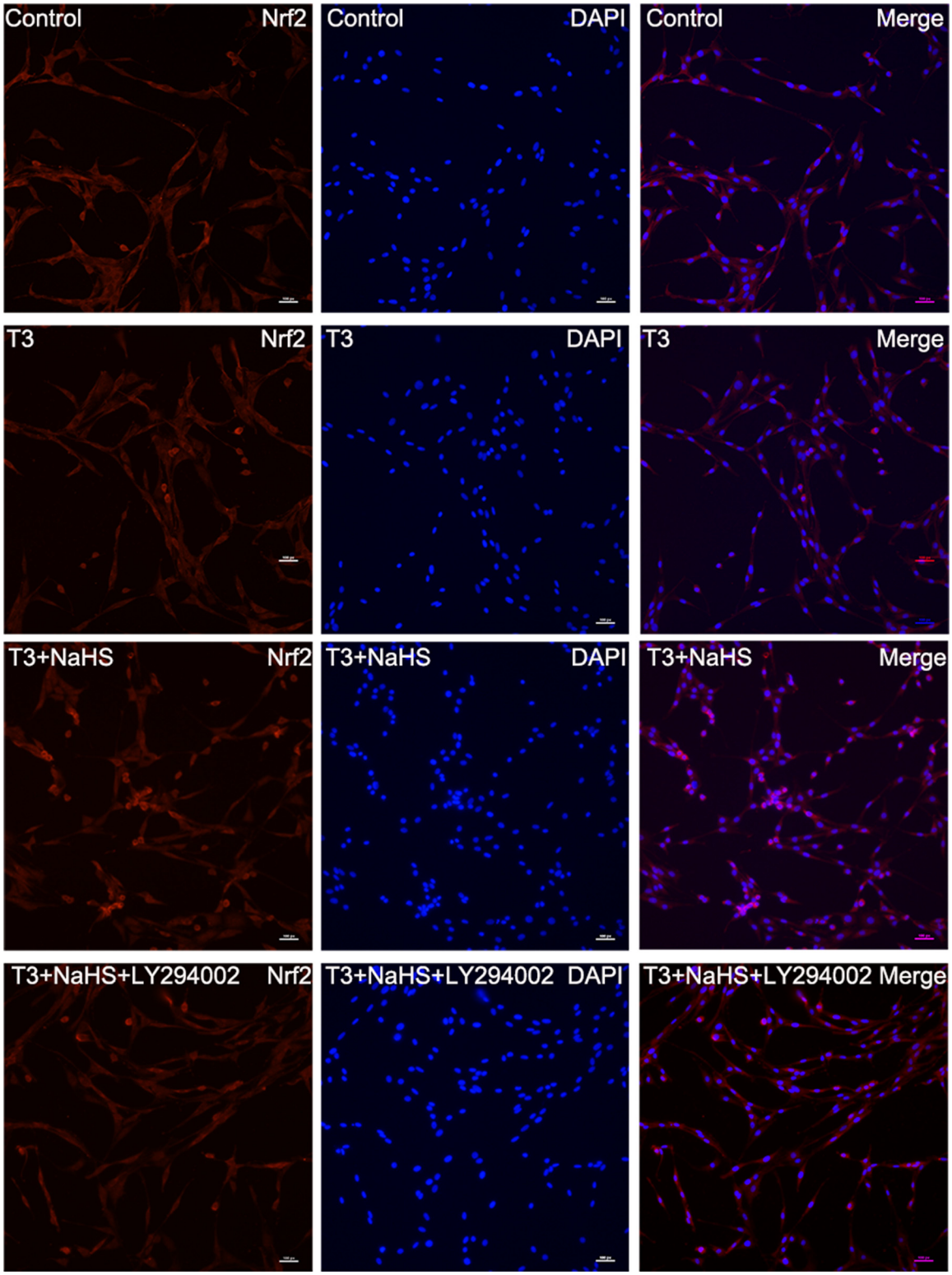

Fig. 8. Effect of hydrogen sulfide on Nrf2 translocation in PC12 cells induced by scratch injury. PC12 cells were induced by scratch test and then examined by immunostaining and microscopy. Nrf2 translocation was evaluated by double Nrf2/DAPI staining. LY294002, as an inhibitor of the PI3K family, were added into the culture media with NaHS, then translocation of Nrf2 from the cytoplasm to nucleus was determined by immunostaining. Representative images from double-stained fluorescent cells (DAPI, blue; Nrf2, red). Scale bars 30 μm.

(Fig. 9).

Our results showed scratch injury significantly decreased cell viability. Because CCK8 measures the metabolic activity of living cells, the data do not verify cell death. To ensure the data is reflecting the cell death instead of decreased metabolic activity. Cytotoxicity lactate dehydrogenase (LDH) assay, which measures LDH released from dead cells, is used to increase the data reliability (Jin et al., 2015; Zhou et al., 2016). LDH is a stable enzyme present in all cell types and is rapidly released into the cell culture medium upon damage of the plasma membrane. Quantification of LDH release is a widely accepted assay for

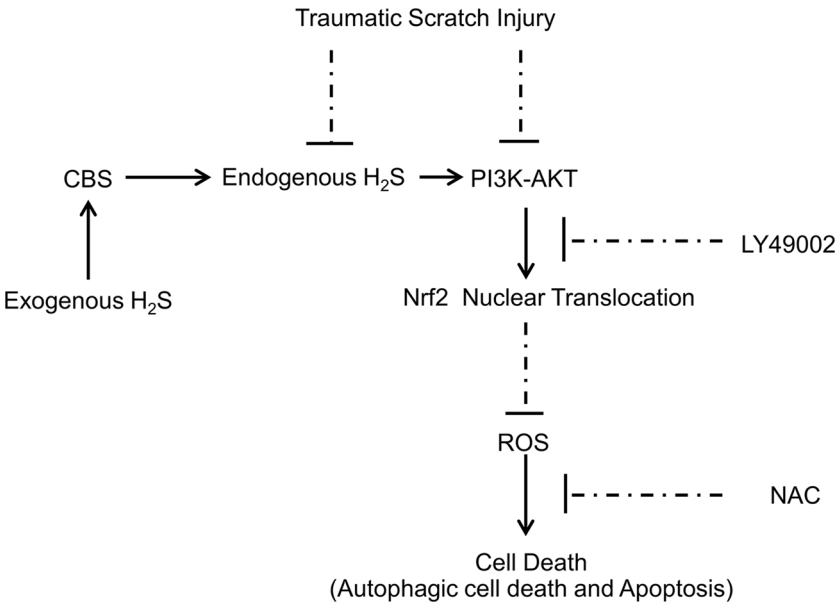

Fig. 9. Hypothetical scheme outlining the mechanisms involved in the protective effects of H_2S on ROS activation and cell death (autophagic cell death and apoptosis) induced by scratch injury. Traumatic scratch injury inhibited the expression of CBS and decreased the production of H_2S in the cell model. H_2S prevents scratch injury-caused oxidative stress and cell death in PC12 cells and nuclear translocation of Nrf2 involves in this protective action of H_2S, which related to the PI3K/AKT dependent signal pathway. NAC (N-acetyl-L-cysteine) is commonly used to identify and test ROS inducers, and to inhibit ROS. Solid lines indicate activation and dotted lines indicate inhibition.

the quantitative determination of cell viability. We have added the LDH assay to avoid the perturbation for the difference of cell numbers between injury and control group. Our results showed that multiple scratch tests resulted in a time-dependent the leakage of LDH from PC12 cells induced by combined the mechanical injury (scratch) with metabolic impairment (no glucose) together (Fig. 1).

ROS generation is considered as a cause of cell death mediated by mitochondrial electron transport chain inhibitors in dopaminergic neuronal cells and PC12 cells (Han and Im, 2008; Shan et al., 2017). Our results showed scratch injury significantly enhanced the production of ROS, altered mitochondrial membrane potential and eventually led to autophagic cell death. Autophagy is the natural, destructive cellular mechanism that degrades damaged proteins and cytoplasm components in lysosomes and thus maintains cellular homeostasis and supplies substrates for energy generation(Wang et al., 2017). Although physiological levels of autophagy are essential for the maintenance of cellular homeostasis during various stress conditions, excessive or uncontrolled levels of autophagy are able to induce autophagy-dependent cell death (Liu and Levine, 2015). Our results indicated that LC3 positive staining was partly colocalized with PI (a cell death marker), implying that a proportion of dying cells were undergoing autophagy, which is one of the mechanisms of scratch-induced injury. Furthermore, NaHS was demonstrated to prevent the scratch-exerted upregulation of LC3 and Beclin-1 expression and downregulation of P62 expression. The present findings suggest that H_2S may be an important protective factor against scratch-induced injury by modulating the autophagic cell death pathway. An increasing number of studies have indicated that H_2S has anti-autophagy effects in the treatment of disease or conditions. Jiang et al found that NaHS treatment reduced cellular injury and suppressed overactivated autophagy induced by OGD/R in PC12 cells (Jiang et al., 2017). Xie et al found that H_2S inhibited autophagic cell death significantly injury via the AKT- mTOR pathway in SCIR (Xie et al., 2017). In addition, other cell death pathway such as apoptosis may also be involved in pathogenesis of scratch-induced injury. Increased production of reactive oxygen species and neuronal apoptosis have also been reported in a scratch injury model (Rao et al., 2015; Zhao et al., 2012). Our previous findings also demonstrated that mitochondrial electron transport chain inhibitors, NaN_3, induced apoptosis in PC12 cells and anti-apoptotic action of H_2S was partly dependent on suppressing the production of ROS (Gao et al., 2018). Both apoptosis and autophagy, evolutionarily-conserved processes that regulate cell fate, are important in the development and normal physiology and in a wide range of diseases (Gump and Thorburn, 2011). The connection between autophagy and apoptosis or other forms of cell death is a burgeoning area of research. In the future, we need to better understand the mechanisms that were discussed here and uncover the interactions between these supposedly separate processes that are surely out there.

Recently, studies showed that Nrf2 (the nuclear factor E2-related factor 2) signaling pathway became a viable treatment option to reduce cellular injury induced by oxidative stress (Jin et al., 2009a, b; Zhang, 2006). The transcription factor Nrf2 is a master regulator transcription factor of cell redox homeostasis in oxidative stress (Kobayashi and Yamamoto, 2006). In the absence of oxidative stress, Nrf2, as a basic leucine zipper redox-sensitive transcription factor, is sequestered in the cytosol by the Keap1 homodimer which acts as a substrate adaptor (Owuor and Kong, 2002). Under conditions of stress or in the presence of Nrf2 activating compounds, this degradation is hindered and Nrf2 translocates to the nucleus. In the nucleus, Nrf2 can bind to the ARE and drive the expression of Nrf2 target genes such as many antioxidant proteins (Mendes Arent et al., 2014). Recent studies have demonstrated that upregulation of Nrf2 activity has attracted an increasing amount of attention as it may provide an alternative therapy for oxidative damage. Several antioxidants have been reported to transcriptionally induce antioxidative enzymes to afford neuroprotection through a Nrf2-dependent mechanism. Zhang et al reported that fucoxanthin attenuated the oxidative stress by increasing the activity of Nrf2 expression in a scratch injury model (Zhang et al., 2017). Xu et al demonstrated that luteolin provided neuroprotective effects through regulation of the Nrf2 pathway in the scratch model in mice primary cultured neurons (Xu et al., 2014). Interest has been directed to the potential value of antioxidant treatment to counteract oxidative stress in brain trauma therapy where oxidative stress has been implied to play a role. Continued research in this area is necessary to enhance our ability to screen potential neuroprotective drugs, to improve understanding of the pathophysiological mechanisms, and to impede the most effective progression of brain trauma.

Hydrogen sulfide (H_2S), previously seen as a noxious gas and an environmental hazard with a rotten egg smell, has been recognized as an endogenous gasotransmitter with importance comparable to nitric oxide (NO) and carbon monoxide (CO), and has attracted increasing attention in recent years (George et al., 2017). In addition to functioning as a signaling molecule in processes such as neuromodulation in the brain, hydrogen sulfide protects neurons from oxidative stress-

induced injury. NaHS, as an inorganic donor of H_2S, has been extensively studied as a neuroprotectant in a variety of neuronal oxidative stress models (Jia et al., 2013; Tay et al., 2010). This gives an idea to assess the therapeutic utility of experimentally tested the donor of H_2S. In order to investigate whether oxidative stress might be involved in TBI-induced neuropathological alterations, we performed ROS assay in PC12 cells injury model whether the existence of ROS scavenger N-acetylcysteine (NAC) or H_2S. NAC is a glutathione (GSH) precursor and shows antioxidant activities. The actions of NAC consist of restoring the antioxidant potential in cells by replenishing the depletion of GSH by free radicals and in scavenging the reactive oxygen species (ROS) (DiNicolantonio et al., 2017; Tardiolo et al., 2018). NAC is an acetylated cysteine compound and a precursor of L-cysteine. L-cysteine is an important natural substrate of H_2S-producing enzymes and NAC as the H_2S-stimulating agent is known to stimulate H_2S production in vivo (Yang et al., 2017). Moreover, NAC was found to suppress leukocyte infiltration in an air pouch model through the generation of endogenous H_2S (Zanardo et al., 2006). We also investigated the glutathione level after scratch injury and found that the decrease of glutathione peroxidase (GSH-Px) and glutathione (GSH) in PC12 cells induced by scratch injury for 24 h was also observed. When H_2S was present in the media, the level of GSH-Px and GSH was significantly increased compared with the injury group. NAC treatment significantly reduced the level of ROS and attenuated ROS-induced cellular injury after scratch injury. Moreover, H_2S has the same antioxidation effect by reducing the production of ROS, weakening mitochondrial damage and cell viability as NAC, suggesting that H_2S may have therapeutic potential against brain damage induced by oxidative stress. Emerging evidence indicates that Nrf2 pathway activation is regarded as a promising new therapeutic way to restore oxidant-antioxidant homeostasis in ROS-mediated neurological disorder (Lim et al., 2014). The important results concerning that H_2S increased the nuclear localization of Nrf2 were observed in mouse embryonic fibroblasts (Yang et al., 2013), in models for cecal ligation and puncture induced sepsis model (Ferlito et al., 2014), uranium-induced acute nephrotoxicity (Zheng et al., 2015) and critical limb ischemia (Islam et al., 2015). In brief, we believe that H_2S-mediated Nrf2 signaling pathway is most likely attributable to the augmentation of intrinsic antioxidant processes in response to oxidative stress. In the experiment, exogenous H_2S donor strongly induced the protein expression of the phosphorylated forms of PI3K and AKT and the nuclear accumulation of Nrf2. LY294002 (an inhibitor of the PI3K family) could effectively suppress the down-regulation of ROS level and the nuclear accumulation of Nrf2 induced by NaHS, which demonstrated NaHS-mediated H_2S generation in regulating the ROS levels at least partly concerned the PI3K/AKT/NRF2 dependent signal pathway. As a cytoprotectant, the fields of H_2S physiology and pharmacology have been rapidly growing in recent years. Although the antioxidant and neuronal cell death inhibition properties of H_2S were thought to be primarily responsible for its biological effects, the underlying mechanisms of H_2S are reflected in other aspects, including acting as regulating protein persulfidation and cyclic nucleotide signaling. It is of interest that the key mechanism underlying H_2S mediated biological effects has been mainly ascribed to the persulfidation of protein by turning cysteine-SH groups to -SSH. For example, H_2S causes the release and nucleus translocation of Nrf2 by persulfidating Keap1 and induction of p66Shc persulfidation (Xie et al., 2014; Yang et al., 2013). Cao and his colleagues reviewed that H_2S played an important role in the regulation of cyclic adenosine monophosphate (cAMP) and cAMP production may lead to altering mitochondrial membrane potential (Acin-Perez et al., 2009; Cao et al., 2017).

In conclusion, H_2S donors are useful tools in studies to elucidate the effects of H_2S on ROS production in acute organ injury and our study using such donor have shown the ability of H_2S to suppress autophagic cell death via reactive oxygen species-mediated signaling pathways in vitro. Our findings also gained new insight into the cellular mechanisms underlying disturbance of endogenous hydrogen sulfide generation and oxidative stress is involved in scratch-induced autophagic cell death in PC12 cells. Although H_2S showed promising effect in scratch-mediated autophagic cell death, research is still underway to determine the exact effects of H_2S as potential drugs in the treatment of brain injury.

Author contributions

MZ, HS, and LT designed the study. JZ, CS, CG, PC, HW, QW and ZW performed experiments and analyzed data. JZ, CG, PC, CL, TW, XC and MZ interpreted data for the work. MZ, HS, XC, and LT wrote the manuscript.

Ethical approval

This article does not contain any studies with human participants or animals performed by any of the authors.

Declaration of Competing Interest

The authors declare that there are no competing interests.

Acknowledgments

This work was supported by the National Natural Science Foundation of China (No.81601306, No.81301039, No.81530062); China Postdoctoral Science Foundation Funded Project (No.2015M570476); The Priority Academic Program Development of Jiangsu Higher Education Institutions (PAPD); Jiangsu Talent Youth Medical Program (QNRC2016245); Shanghai Key Lab of Forensic Medicine (KF1801); Suzhou Science and Technology Development Project (SYS2018082), and the Fifth Batch of Gusu District Health Talent Training Project (GSWS2019060).

References

Acin-Perez, R., Salazar, E., Kamenetsky, M., Buck, J., Levin, L.R., Manfredi, G., 2009. Cyclic AMP produced inside mitochondria regulates oxidative phosphorylation. Cell Metab. 9 (3), 265–276.

Baez-Jurado, E., Vega, G.G., Aliev, G., Tarasov, V.V., Esquinas, P., Echeverria, V., Barreto, G.E., 2017. Blockade of neuroglobin reduces protection of conditioned medium from human mesenchymal stem cells in human astrocyte model (T98G) under a scratch assay. Mol. Neurobiol.

Brooks, J.C., Strauss, D.J., Shavelle, R.M., Paculdo, D.R., Hammond, F.M., Harrison-Felix, C.L., 2013. Long-term disability and survival in traumatic brain injury: results from the National Institute on Disability and Rehabilitation Research Model Systems. Arch. Phys. Med. Rehabil. 94 (11), 2203–2209.

Cao, X., Wu, Z., Xiong, S., Cao, L., Sethi, G., Bian, J.S., 2017. The role of hydrogen sulfide in cyclic nucleotide signaling. Biochem. Pharmacol.

Chang, R., Zhou, R., Qi, X., Wang, J., Wu, F., Yang, W., Zhang, W., Sun, T., Li, Y., Yu, J., 2016. Protective effects of aloin on oxygen and glucose deprivation-induced injury in PC12 cells. Brain Res. Bull. 121, 75–83.

DiNicolantonio, J.J., JH, O.K., McCarty, M.F., 2017. Boosting endogenous production of vasoprotective hydrogen sulfide via supplementation with taurine and N-acetylcysteine: a novel way to promote cardiovascular health. Open Heart 4 (1), e000600.

Enokido, Y., Suzuki, E., Iwasawa, K., Namekata, K., Okazawa, H., Kimura, H., 2005. Cystathionine beta-synthase, a key enzyme for homocysteine metabolism, is preferentially expressed in the radial glia/astrocyte lineage of developing mouse CNS. FASEB J. 19 (13), 1854–1856.

Etienne-Manneville, S., Hall, A., 2001. Integrin-mediated activation of Cdc42 controls cell polarity in migrating astrocytes through PKCzeta. Cell 106 (4), 489–498.

Faden, A.I., Movsesyan, V.A., Knoblach, S.M., Ahmed, F., Cernak, I., 2005. Neuroprotective effects of novel small peptides in vitro and after brain injury. Neuropharmacology 49 (3), 410–424.

Ferlito, M., Wang, Q., Fulton, W.B., Colombani, P.M., Marchionni, L., Fox-Talbot, K., Paolocci, N., Steenbergen, C., 2014. Hydrogen sulfide [corrected] increases survival during sepsis: protective effect of CHOP inhibition. J. Immunol. 192 (4), 1806–1814.

Gao, C., Chang, P., Yang, L., Wang, Y., Zhu, S., Shan, H., Zhang, M., Tao, L., 2018. Neuroprotective effects of hydrogen sulfide on sodium azide-induced oxidative stress in PC12 cells. Int. J. Mol. Med. 41 (1), 242–250.

Gao, K., Wang, C.R., Jiang, F., Wong, A.Y., Su, N., Jiang, J.H., Chai, R.C., Vatcher, G., Teng, J., Chen, J., Jiang, Y.W., Yu, A.C., 2013. Traumatic scratch injury in astrocytes triggers calcium influx to activate the JNK/c-Jun/AP-1 pathway and switch on GFAP expression. Glia 61 (12), 2063–2077.

George, A.K., Behera, J., Kelly, K.E., Zhai, Y., Tyagi, N., 2017. Hydrogen sulfide, endoplasmic reticulum stress and alcohol mediated neurotoxicity. Brain Res. Bull. 130,

251–256.
Gump, J.M., Thorburn, A., 2011. Autophagy and apoptosis: what is the connection? Trends Cell Biol. 21 (7), 387–392.
Han, M., Im, D.S., 2008. Effects of mitochondrial inhibitors on cell viability in U937 monocytes under glucose deprivation. Arch. Pharm. Res. 31 (6), 749–757.
Huang, C.W., Moore, P.K., 2015. H2S synthesizing enzymes: biochemistry and molecular aspects. Handb. Exp. Pharmacol. 230, 3–25.
Huang, S., Ge, X., Yu, J., Han, Z., Yin, Z., Li, Y., Chen, F., Wang, H., Zhang, J., Lei, P., 2018. Increased miR-124-3p in microglial exosomes following traumatic brain injury inhibits neuronal inflammation and contributes to neurite outgrowth via their transfer into neurons. FASEB J. 32 (1), 512–528.
Ishigami, M., Hiraki, K., Umemura, K., Ogasawara, Y., Ishii, K., Kimura, H., 2009. A source of hydrogen sulfide and a mechanism of its release in the brain. Antioxid. Redox Signal. 11 (2), 205–214.
Islam, K.N., Polhemus, D.J., Donnarumma, E., Brewster, L.P., Lefer, D.J., 2015. Hydrogen sulfide levels and nuclear factor-erythroid 2-Related factor 2 (NRF2) activity are attenuated in the setting of critical limb ischemia (CLI). J. Am. Heart Assoc. 4 (5).
Jha, S., Calvert, J.W., Duranski, M.R., Ramachandran, A., Lefer, D.J., 2008. Hydrogen sulfide attenuates hepatic ischemia-reperfusion injury: role of antioxidant and anti-apoptotic signaling. Am. J. Physiol. Heart Circ. Physiol. 295 (2), H801–806.
Jia, J., Xiao, Y., Wang, W., Qing, L., Xu, Y., Song, H., Zhen, X., Ao, G., Alkayed, N.J., Cheng, J., 2013. Differential mechanisms underlying neuroprotection of hydrogen sulfide donors against oxidative stress. Neurochem. Int. 62 (8), 1072–1078.
Jiang, W.W., Huang, B.S., Han, Y., Deng, L.H., Wu, L.X., 2017. Sodium hydrosulfide attenuates cerebral ischemia/reperfusion injury by suppressing overactivated autophagy in rats. FEBS Open Bio 7 (11), 1686–1695.
Jin, S.F., Ma, H.L., Liu, Z.L., Fu, S.T., Zhang, C.P., He, Y., 2015. XL413, a cell division cycle 7 kinase inhibitor enhanced the anti-fibrotic effect of pirfenidone on TGF-beta1-stimulated C3H10T1/2 cells via Smad2/4. Exp. Cell Res. 339 (2), 289–299.
Jin, W., Wang, H., Yan, W., Zhu, L., Hu, Z., Ding, Y., Tang, K., 2009a. Role of Nrf2 in protection against traumatic brain injury in mice. J. Neurotrauma 26 (1), 131–139.
Jin, W., Wang, H.D., Hu, Z.G., Yan, W., Chen, G., Yin, H.X., 2009b. Transcription factor Nrf2 plays a pivotal role in protection against traumatic brain injury-induced acute intestinal mucosal injury in mice. J. Surg. Res. 157 (2), 251–260.
Kobayashi, M., Yamamoto, M., 2006. Nrf2-Keap1 regulation of cellular defense mechanisms against electrophiles and reactive oxygen species. Adv. Enzyme Regul. 46, 113–140.
Lee, M., Schwab, C., Yu, S., McGeer, E., McGeer, P.L., 2009. Astrocytes produce the antiinflammatory and neuroprotective agent hydrogen sulfide. Neurobiol. Aging 30 (10), 1523–1534.
Lee, S.W., Hu, Y.S., Hu, L.F., Lu, Q., Dawe, G.S., Moore, P.K., Wong, P.T., Bian, J.S., 2006. Hydrogen sulphide regulates calcium homeostasis in microglial cells. Glia 54 (2), 116–124.
Lim, J.L., Wilhelmus, M.M., de Vries, H.E., Drukarch, B., Hoozemans, J.J., van Horssen, J., 2014. Antioxidative defense mechanisms controlled by Nrf2: state-of-the-art and clinical perspectives in neurodegenerative diseases. Arch. Toxicol. 88 (10), 1773–1786.
Liu, Y., Levine, B., 2015. Autosis and autophagic cell death: the dark side of autophagy. Cell Death Differ. 22 (3), 367–376.
Loov, C., Shevchenko, G., Geeyarpuram Nadadhur, A., Clausen, F., Hillered, L., Wetterhall, M., Erlandsson, A., 2013. Identification of injury specific proteins in a cell culture model of traumatic brain injury. PLoS One 8 (2), e55983.
Ma, J., Shui, S., Han, X., Guo, D., Li, T., Yan, L., 2016. microRNA-22 attenuates neuronal cell apoptosis in a cell model of traumatic brain injury. Am. J. Transl. Res. 8 (4), 1895–1902.
Ma, Y.H., Zeng, X., Zhang, K., Zeng, Y.S., 2012. A new in vitro injury model of mouse neurons induced by mechanical scratching. Neurosci. Lett. 510 (1), 14–19.
Mendes Arent, A., de Souza, L.F., Walz, R., Dafre, A.L., 2014. Perspectives on molecular biomarkers of oxidative stress and antioxidant strategies in traumatic brain injury. Biomed Res. Int. 2014, 723060.
Miyamoto, R., Otsuguro, K., Yamaguchi, S., Ito, S., 2014. Contribution of cysteine aminotransferase and mercaptopyruvate sulfurtransferase to hydrogen sulfide production in peripheral neurons. J. Neurochem. 130 (1), 29–40.
Morrison 3rd, B., Elkin, B.S., Dolle, J.P., Yarmush, M.L., 2011. In vitro models of traumatic brain injury. Annu. Rev. Biomed. Eng. 13, 91–126.
Owuor, E.D., Kong, A.N., 2002. Antioxidants and oxidants regulated signal transduction pathways. Biochem. Pharmacol. 64 (5–6), 765–770.
Qu, K., Lee, S.W., Bian, J.S., Low, C.M., Wong, P.T., 2008. Hydrogen sulfide: neurochemistry and neurobiology. Neurochem. Int. 52 (1–2), 155–165.
Rao, W., Zhang, L., Peng, C., Hui, H., Wang, K., Su, N., Wang, L., Dai, S.H., Yang, Y.F., Chen, T., Luo, P., Fei, Z., 2015. Downregulation of STIM2 improves neuronal survival after traumatic brain injury by alleviating calcium overload and mitochondrial dysfunction. Biochim. Biophys. Acta 1852 (11), 2402–2413.
Robert, K., Vialard, F., Thiery, E., Toyama, K., Sinet, P.M., Janel, N., London, J., 2003. Expression of the cystathionine beta synthase (CBS) gene during mouse development and immunolocalization in adult brain. J. Histochem. Cytochem. 51 (3), 363–371.
Shan, H., Chu, Y., Chang, P., Yang, L., Wang, Y., Zhu, S., Zhang, M., Tao, L., 2017. Neuroprotective effects of hydrogen sulfide on sodium azideinduced autophagic cell death in PC12 cells. Mol. Med. Rep. 16 (5), 5938–5946.
Shefa, U., Yeo, S.G., Kim, M.S., Song, I.O., Jung, J., Jeong, N.Y., Huh, Y., 2017. Role of gasotransmitters in oxidative stresses, neuroinflammation, and neuronal repair. Biomed. Res. Int. 2017, 1689341.
Shen, Q., Hiebert, J.B., Hartwell, J., Thimmesch, A.R., Pierce, J.D., 2016. Systematic review of traumatic brain injury and the impact of antioxidant therapy on clinical outcomes. Worldviews Evid. Nurs. 13 (5), 380–389.
Tang, X.Q., Fan, L.L., Li, Y.J., Shen, X.T., Zhuan, Y.Y., He, J.Q., Xu, J.H., Hu, B., Li, Y.J., 2011. Inhibition of hydrogen sulfide generation contributes to 1-methy-4-phenylpyridinium ion-induced neurotoxicity. Neurotox. Res. 19 (3), 403–411.
Tang, X.Q., Fang, H.R., Zhou, C.F., Zhuang, Y.Y., Zhang, P., Gu, H.F., Hu, B., 2013. A novel mechanism of formaldehyde neurotoxicity: inhibition of hydrogen sulfide generation by promoting overproduction of nitric oxide. PLoS One 8 (1), e54829.
Tardiolo, G., Bramanti, P., Mazzon, E., 2018. Overview on the effects of N-Acetylcysteine in neurodegenerative diseases. Molecules 23 (12).
Tay, A.S., Hu, L.F., Lu, M., Wong, P.T., Bian, J.S., 2010. Hydrogen sulfide protects neurons against hypoxic injury via stimulation of ATP-sensitive potassium channel/protein kinase C/extracellular signal-regulated kinase/heat shock protein 90 pathway. Neuroscience 167 (2), 277–286.
Torrente, D., Avila, M.F., Cabezas, R., Morales, L., Gonzalez, J., Samudio, I., Barreto, G.E., 2014. Paracrine factors of human mesenchymal stem cells increase wound closure and reduce reactive oxygen species production in a traumatic brain injury in vitro model. Hum. Exp. Toxicol. 33 (7), 673–684.
Wang, S.S., Chen, Y.H., Chen, N., Wang, L.J., Chen, D.X., Weng, H.L., Dooley, S., Ding, H.G., 2017. Hydrogen sulfide promotes autophagy of hepatocellular carcinoma cells through the PI3K/Akt/mTOR signaling pathway. Cell Death Dis. 8 (3), e2688.
Wang, X.Y., Yang, H.W., 2016. Upregulation of CBS/H2S system contributes to asymmetric dimethylarginine-triggered protection against the neurotoxicity of glutamate to PC12 cells by inhibiting NOS/NO pathway. Exp. Cell Res. 346 (1), 111–118.
Xie, L., Yu, S., Yang, K., Li, C., Liang, Y., 2017. Hydrogen sulfide inhibits autophagic neuronal cell death by reducing oxidative stress in spinal cord ischemia reperfusion injury. Oxid. Med. Cell. Longev. 2017, 8640284.
Xie, Z.Z., Shi, M.M., Xie, L., Wu, Z.Y., Li, G., Hua, F., Bian, J.S., 2014. Sulfhydration of p66Shc at cysteine59 mediates the antioxidant effect of hydrogen sulfide. Antioxid. Redox Signal. 21 (18), 2531–2542.
Xu, J., Wang, H., Ding, K., Zhang, L., Wang, C., Li, T., Wei, W., Lu, X., 2014. Luteolin provides neuroprotection in models of traumatic brain injury via the Nrf2-ARE pathway. Free Radic. Biol. Med. 71, 186–195.
Yan, J.W., Tan, T.Y., Huang, Q.L., 2013. Protective effect of astrocyte-conditioned medium on neurons following hypoxia and mechanical injury. Chin. J. Traumatol. 16 (1), 3–9.
Yang, C.T., Chen, L., Xu, S., Day, J.J., Li, X., Xian, M., 2017. Recent development of hydrogen sulfide Releasing/Stimulating reagents and their potential applications in Cancer and glycometabolic disorders. Front. Pharmacol. 8, 664.
Yang, G., Zhao, K., Ju, Y., Mani, S., Cao, Q., Puukila, S., Khaper, N., Wu, L., Wang, R., 2013. Hydrogen sulfide protects against cellular senescence via S-sulfhydration of Keap1 and activation of Nrf2. Antioxid. Redox Signal. 18 (15), 1906–1919.
Yu, A.C., Lee, Y.L., Eng, L.F., 1993. Astrogliosis in culture: I. The model and the effect of antisense oligonucleotides on glial fibrillary acidic protein synthesis. J. Neurosci. Res. 34 (3), 295–303.
Zanardo, R.C., Brancaleone, V., Distrutti, E., Fiorucci, S., Cirino, G., Wallace, J.L., 2006. Hydrogen sulfide is an endogenous modulator of leukocyte-mediated inflammation. FASEB J. 20 (12), 2118–2120.
Zhang, D.D., 2006. Mechanistic studies of the Nrf2-Keap1 signaling pathway. Drug Metab. Rev. 38 (4), 769–789.
Zhang, L., Wang, H., Fan, Y., Gao, Y., Li, X., Hu, Z., Ding, K., Wang, Y., Wang, X., 2017. Fucoxanthin provides neuroprotection in models of traumatic brain injury via the Nrf2-ARE and Nrf2-autophagy pathways. Sci. Rep. 7, 46763.
Zhang, M., Shan, H., Chang, P., Ma, L., Chu, Y., Shen, X., Wu, Q., Wang, Z., Luo, C., Wang, T., Chen, X., Tao, L., 2017a. Upregulation of 3-MST relates to neuronal autophagy after traumatic brain injury in mice. Cell. Mol. Neurobiol. 37 (2), 291–302.
Zhang, M., Shan, H., Chang, P., Wang, T., Dong, W., Chen, X., Tao, L., 2014. Hydrogen sulfide offers neuroprotection on traumatic brain injury in parallel with reduced apoptosis and autophagy in mice. PLoS One 9 (1), e87241.
Zhang, M., Shan, H., Wang, T., Liu, W., Wang, Y., Wang, L., Zhang, L., Chang, P., Dong, W., Chen, X., Tao, L., 2013. Dynamic change of hydrogen sulfide after traumatic brain injury and its effect in mice. Neurochem. Res. 38 (4), 714–725.
Zhang, M., Wu, X., Xu, Y., He, M., Yang, J., Li, J., Li, Y., Ao, G., Cheng, J., Jia, J., 2017b. The cystathionine beta-synthase/hydrogen sulfide pathway contributes to microglia-mediated neuroinflammation following cerebral ischemia. Brain Behav. Immun. 66, 332–346.
Zhao, Y., Luo, P., Guo, Q., Li, S., Zhang, L., Zhao, M., Xu, H., Yang, Y., Poon, W., Fei, Z., 2012. Interactions between SIRT1 and MAPK/ERK regulate neuronal apoptosis induced by traumatic brain injury in vitro and in vivo. Exp. Neurol. 237 (2), 489–498.
Zheng, J., Zhao, T., Yuan, Y., Hu, N., Tang, X., 2015. Hydrogen sulfide (H2S) attenuates uranium-induced acute nephrotoxicity through oxidative stress and inflammatory response via Nrf2-NF-kappaB pathways. Chem. Biol. Interact. 242, 353–362.
Zhou, D., Li, B.H., Wang, J., Ding, Y.N., Dong, Y., Chen, Y.W., Fan, J.G., 2016. Prolyl oligopeptidase inhibition attenuates steatosis in the L02 human liver cell line. PLoS One 11 (10), e0165224.
Zhu, Z., Zhang, Q., Yu, Z., Zhang, L., Tian, D., Zhu, S., Bu, B., Xie, M., Wang, W., 2007. Inhibiting cell cycle progression reduces reactive astrogliosis initiated by scratch injury in vitro and by cerebral ischemia in vivo. Glia 55 (5), 546–558.